

Original Article

Clinical correlation and diagnostic value of circular RNA determined via next-generation sequencing in lung squamous cell carcinomas

Fei Xu^{1,2}, Yang Liu⁴, Yu Dai², Chun-Sheng Li³, Chun-Sun Li², Yan Chang⁵, Yong-Fu Ma⁴, Yun-Jing Li⁴, Liang-An Chen^{1,2}

¹Medical School, Nankai University, Tianjin, P.R. China; Departments of ²Respiratory Medicine, ⁴Thoracic Surgery, Chinese People's Liberation Army General Hospital, Beijing, P.R. China; ³Beijing Municipal Public Security Bureau Haidian Sub-Bureau, Beijing, P.R. China; ⁵Chinese People's Liberation Army of Rocket Force General Hospital, Beijing, P.R. China

Received March 25, 2018; Accepted July 7, 2018; Epub November 15, 2018; Published November 30, 2018

Abstract: There are investigations suggesting that circular RNAs (circRNAs) may play a critical role in tumor progression, and that their identification could serve as novel biomarkers to improve cancer diagnosis. In this study, we proposed to investigate the landscape of circRNAs in lung squamous cell carcinomas (LSCCs) and to identify those that can aid in lung cancer (LC) diagnosis. The circRNA expression landscape and its functional assessments were profiled in five surgical LSCCs along with five paired adjacent normal tissues via next-generation sequencing (RNA-seq) and bioinformatics technology. Correlations were explored between expression levels of validated circRNAs and clinical features of participants. ROC curves and AUC were constructed to evaluate the diagnostic values. Among 256 co-differentially expressed circRNAs (co-DE circRNAs) in LSCCs with paired samples, there were 15 significantly co-upregulated and 93 significantly co-downregulated DE circRNAs. The GO function prediction analyses showed that protein binding, intracellular, and metabolic process were the top three functions of circRNA parental genes. Adherens junctions, lysine degradation, and ErbB signaling pathway were the three most enriched pathways according to KEGG pathway assessment. Of five predicted co-DE circRNAs, including *circLIFR*, *circBRAF*, *circPTPRM*, *circEPB41L2*, and *circPVT1*, four co-DE circRNAs except *circPVT1* were identified by qRT-PCR with Sanger sequencing in 86 samples (43 surgical LCs with 43 paired adjacent normal tissues). Furthermore, *circLIFR*, *circBRAF*, *circPTPRM*, and *circEPB41L2* were significantly associated with pathological subtypes, which had a statistical discrepancy regarding LSCCs discriminated from lung adenocarcinomas. *CircLIFR* and *circEPB41L2* were also negatively correlated with blood SCC. ROC curves showed that *circLIFR* exhibited the highest AUC value (0.871) in LCs with corresponding high sensitivity and specificity (0.744 and 0.884), and *circEPB41L2* had the highest AUC value (0.947) in LSCCs with higher sensitivity (0.867) and specificity (0.947). Combination of these four co-DE circRNAs did not present a high AUC value (AUC: 0.871 in LCs; 0.937 in LSCCs), without corresponding increase in sensitivity (0.767 in LCs, 0.933 in LSCCs) and specificity (0.837 in LCs, 0.867 in LSCCs). This study highlights downregulated four circRNAs (*circLIFR*, *circBRAF*, *circPTPRM*, and *circEPB41L2*) that might be promising diagnostic biomarkers for LCs, with *circEPB41L2* being the best diagnostic biomarker for LSCCs.

Keywords: Circular RNA, lung cancer, lung squamous cell carcinomas, clinical characteristics, diagnosis

Introduction

Lung cancer (LC) is the leading cause of cancer deaths worldwide with a low 5-year overall survival rate of approximately 15% [1, 2]. There are two main pathological subtypes of LC, namely small cell lung cancer (SCLC) and non-small cell lung cancer (NSCLC), which mainly include lung adenocarcinoma (LADC), lung squamous cell carcinoma (LSCC), and large-cell carcinoma

(LCC). Available investigations showed that several tumor biomarkers were associated with histological types with significantly higher levels of carcinoembryonic antigen (CEA) in LADC, squamous cell carcinoma antigen (SCC) and cytokeratin 19 fragment (CYFRA21-1) in LSCC, and neuron-specific enolase (NSE) in SCLC [3]. However, these known biomarkers are insufficient for early diagnosis in LC patients due to the relatively low specificity and sensitivity [3, 4].

Circular RNA (circRNA) is a type of endogenous non-coding RNA with a covalently closed loop, stability, and widespread distribution, and it typically exists in the cytoplasm, cell nucleus, or exosomes. According to current studies, circRNA may be involved in multiple biological and pathophysiological processes, such as the regulation of cell behavior [5], gene transcription [6] and expression, interaction with proteins by serving as absorbing microRNA sponges [7-9], regulating or binding proteins [5, 6], encoding peptides [10], protein translation [11], and signaling pathway modulation [12, 13]. Consequently, circRNA dysregulation may play an important role in disease development and progression, especially cancer [14, 15]. Under the help of high-throughput sequencing of RNA (RNA-seq) and bioinformatics technologies, tremendous numbers of circRNAs have been identified and determined to be expressed specifically and differently in various cancer cell lines [12, 16, 17], cancer tissues [12, 13, 16-20], plasma [18], and exosomes [21]. Abundant circRNAs have also been confirmed in various types of cancer, including hepatocellular carcinoma [13], colorectal or gastric cancer [18, 20], gliomas [22], breast cancer [16], and esophageal squamous cell carcinoma [17], suggesting that circRNAs could be novel biomarkers for cancer diagnosis. However, the underlying characteristics of circRNAs remain largely unknown, especially in LC. A recent study [12] showed that *circ-ITCH* inhibits LC progression in both tissues and cell lines via suppressing the proliferation of LC cells as sponges of miR-7 and miR-214 and inhibiting Wnt/ β -catenin signal transduction.

In this study, we proposed to portray the expression profile of circRNAs and assess their functions in human LSCCs through RNA-seq and analyze the differential expression of validated circRNAs correlating with clinical characteristics to further study whether circRNAs can serve as biomarkers for lung cancer diagnosis.

Materials and methods

Human paired specimens

Eighty-six specimens (43 lung tumor and 43 adjacent normal paired tissues) were acquired on patients who were diagnosed with primary LC at the pathology department of Chinese PLA general hospital and underwent surge-

ries. None of the patients received preoperative chemotherapy or radiotherapy. All isolated lung specimens were placed in liquid nitrogen within half an hour. With written informed consent, patient demographic information and other lab test information were collected, including gender, age, smoking status, cancer family, TNM^{8th}, and blood biomarkers (blood CEA, SCC, CYFRA21-1, and NSE). The study was approved by the Clinical Research Ethics Committee of the Chinese PLA General Hospital.

RNA-seq analysis

RNA isolation, library preparation, and circRNA sequencing: Total RNA (no less than 3 μ g) from each of the 10 samples (5 LSCCs and 5 adjacent normal paired tissues) was isolated using TRIzol reagent (Life Technologies, Carlsbad, CA, USA). RNA quantification and qualification were certified as follows: RNA degradation and contamination were checked using the NanoPhotometer[®] spectrophotometer (Implen, Westlake Village, CA, USA) and on 1% agarose gels. Furthermore, RNA concentration and integrity were assessed using Qubit[®] RNA Assay Kit in the Qubit[®] 2.0 Fluorometer (Life Technologies) and RNA Nano 6000 Assay Kit of the Bioanalyzer 2100 system (Agilent Technologies, Santa Clara, CA, USA).

Ribosomal RNA (rRNA) was removed using Epicentre Ribo-zero[™] rRNA Removal Kit (Epicentre, Madison, WI, USA) and cleaned via ethanol precipitation to construct RNA-seq libraries in advance. Strand-specific sequencing libraries were generated using the rRNA-depleted RNA from the NEBNext[®] Ultra[™] Directional RNA Library Prep Kit for Illumina[®] (NEB, Ipswich, MA, USA) following the manufacturer's recommendations. Briefly, the first- and second-strand complementary DNAs (cDNAs) were synthesized with random hexamer primers after fragmentation of ribosome-depleted RNA. dTTP in the dNTPs was replaced by dUTP in the reaction buffer for the second-strand cDNA synthesis. After the adenylation of the 3' ends of DNA fragments, NEBNext Adaptor with hairpin loop structure was ligated to prepare for hybridization. Thereafter, the size-selected and adaptor-selected library fragments preferentially 150-250 bp in length were chosen by 3 μ L USER Enzyme (NEB) and purified with the AMPure XP system (Beckman Coulter, Brea, CA, USA) before polymerase chain reaction (PCR). PCR

Circular RNA for lung squamous cell carcinomas diagnosis

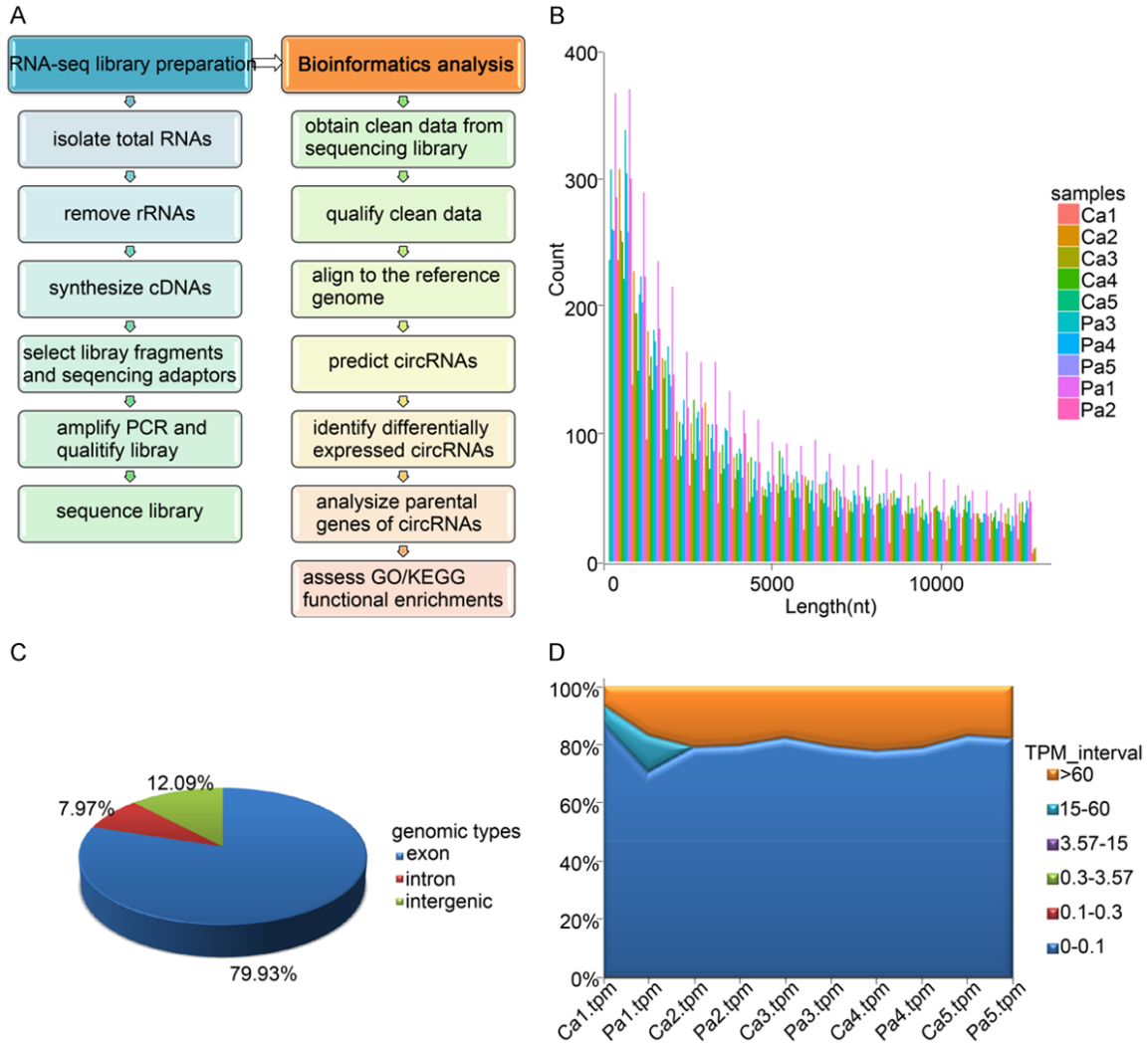


Figure 1. The landscape of circRNAs in 10 samples (five LSCCs and five adjacent normal paired tissues). A. Flow diagram of profiling of circRNAs via RNA-seq and bioinformatics. B. Histogram presenting the length distribution of circRNAs in each sample. The median length was 998 nt. C. Parental genome origin of inferred circRNAs in 10 samples. D. The normalized expression of putative circRNAs using Read count_TPM. Read count_TPM were 0-0.1 transcripts per million reads accounting for nearly more than 80% of circRNAs.

amplification was performed with Phusion High-Fidelity DNA Polymerase, Universal PCR Primers, and Index (X) Primer, and products were subsequently purified using the AMPure XP system. Finally, the quality of the libraries was assessed using the Agilent Bioanalyzer 2100 system. The libraries were sequenced on the Illumina HiSeq 2500 platform with the generation of 125-bp paired-end reads, after clustering the index-coded samples on a cBot Cluster Generation System using TruSeq PE Cluster Kit v3-cBot-HS (Illumina, San Diego, CA, USA). RNA-seq was operated by next-generation and high-throughput sequencing (**Figure 1A**).

Identification and quantification of inferred circRNAs in LSCCs: The clean data (clean reads) of RNA-seq were obtained by removing reads containing adaptor or poly-N and low-quality reads from raw data (FASTQ format) processed through in-house Perl scripts. All the downstream analyses were performed on the basis of the clean data with high quality calculated by Q20, Q30, and GC content. Then, the index of the reference genome was built using Bowtie v2.0.6 [23], and paired-end clean data were mapped or aligned to the reference genome (GRCh37/hg38) from the UCSC genome database (<http://genome.ucsc.edu/>) using TopHat v2.0.9 [24]. The unmapped reads were used to

Circular RNA for lung squamous cell carcinomas diagnosis

Table 1. Primers of circRNAs and GAPDH for qRT-PCR

Name or ID	Primer Sequence
GAPDH	Forward CATGAGAAGTATGACAACAGCCT
	Reverse AGTCCTTCCACGATACCAAAGT
hsa_circ_0001821	Forward GCTGGGCTTGAGGCCTGAT
	Reverse CCAGACCACTGAAGATCACTG
hsa_circ_0072309	Forward GGAGCTCGTAAAATTAGACTG
	Reverse AATGTTGATAACAGCCACTGGA
hsa_circ_0006114	Forward TGCCAGCTTATGAACCTTGAGAC
	Reverse TGTTTGAGTTGGTTCTCTCCAC
hsa_circ_0006460	Forward AAGCCACAACCTGGCTATTGTTA
	Reverse TCTCGTTGCCAAATTGATT
hsa_circ_0077837	Forward CATGCCAAGGGACAAGTGTAT
	Reverse TTGCATCTGTTCTAACTGGCT

identify circRNAs as previously described, denoted as “find_circ” [25]. In brief, the unmapped reads were processed to 20-nucleotide anchors from both ends of the read. Anchors that aligned in the reverse orientation (head-to-tail) indicated (represent) a back-spliced junction. Anchor alignments were extended in a way so that the complete read aligned and the breakpoint was flanked by a GT/AG splice site. Read counts no less than two were ascertained as predicted circRNAs. Known circRNAs were annotated according to circBase website (<http://www.circbase.org/>) to distinguish novel circRNAs.

The total read count that spanned back-spliced junctions was used as an absolute measure of circRNA abundance. The normalized relative expression of one circRNA was estimated by denoted TPM (i.e., transcripts per million reads) [26]. In short, TPM_read count = circular read count*1,000,000/sum of read count. The genomic regions that were mapped to predict circRNAs were annotated according to RefSeq and UCSC Known Genes databases [37]. The corresponding genes of transcript fragments as the parental genes of circRNAs were determined via a custom script that identified the longest transcript fragment whose boundaries (5' end or 3' end) exactly matched both ends of the circRNA in the same strand.

Identification of differentially expressed circRNAs and their functional assessment: Differential expression (diff_expression) of circRNAs (DE_circRNAs) in all paired samples was determined via DESeq2, a model based on the negative binomial distribution [27]. Transcripts with

adjusted *P*-value (*q*-value) less than 0.05 and $|\log_2^{\text{(foldchange)}}|$ more than 1 were assigned as statistical diff_expression. Gene Ontology (GO, <http://www.geneontology.org/>) enrichment analysis of parental genes of DE_circRNAs was implemented by the Goseq R package, via Wallenius non-central hypergeometric distribution in which the gene length bias was corrected [28]. Kyoto Encyclopedia of Genes and Genomes (KEGG) pathway (<http://www.genome.jp/kegg/>) was used to systematically understand the putative functions of the biological system of the parental genes of circRNAs via KOBAS software [29, 30]. The GO terms or KEGG pathways with *q*-values less than 0.05 were considered significantly enriched by differentially expressed genes.

qRT-PCR of inferred circRNAs in lung cancer samples with Sanger sequencing

The total RNA from 86 samples (43 LC and 43 adjacent normal paired tissues) was isolated with DNA elimination using TRIzol (Life Technologies) and DNase I. cDNA was synthesized with the PrimeScript RT Master Mix (Takara, Dalian, China) with 1 µg RNA from each sample. To quantify the inferred circRNAs, real-time quantitative PCR (qPCR) was performed using SYBR Premix Ex Taq II (Takara). In particular, divergent primers annealing at the distal ends (or spanning the cyclization site) of circRNAs were used to determine the abundance of circRNAs, and *GAPDH* was used as an internal standard. Sanger sequencing was performed to identify the specificity of each circRNA primer and the cyclization sites (**Table 1** and **Supplementary Figure 1**). The relative expression of circRNAs was calculated using the $2^{-\Delta\Delta Ct}$ method [31].

Statistical analysis

Statistic analysis and graph were performed using IBM SPSS22.0 and GraphPad Prism 6.0. The underlying association between the inferred circRNAs and the clinical characteristics of the participants were analyzed and computed using the Pearson or Spearman coefficients, as appropriate. The comparisons between two or more groups were assessed using the Student's *t*-test or one-way analysis of variance, as appropriate. The receiver operat-

Circular RNA for lung squamous cell carcinomas diagnosis

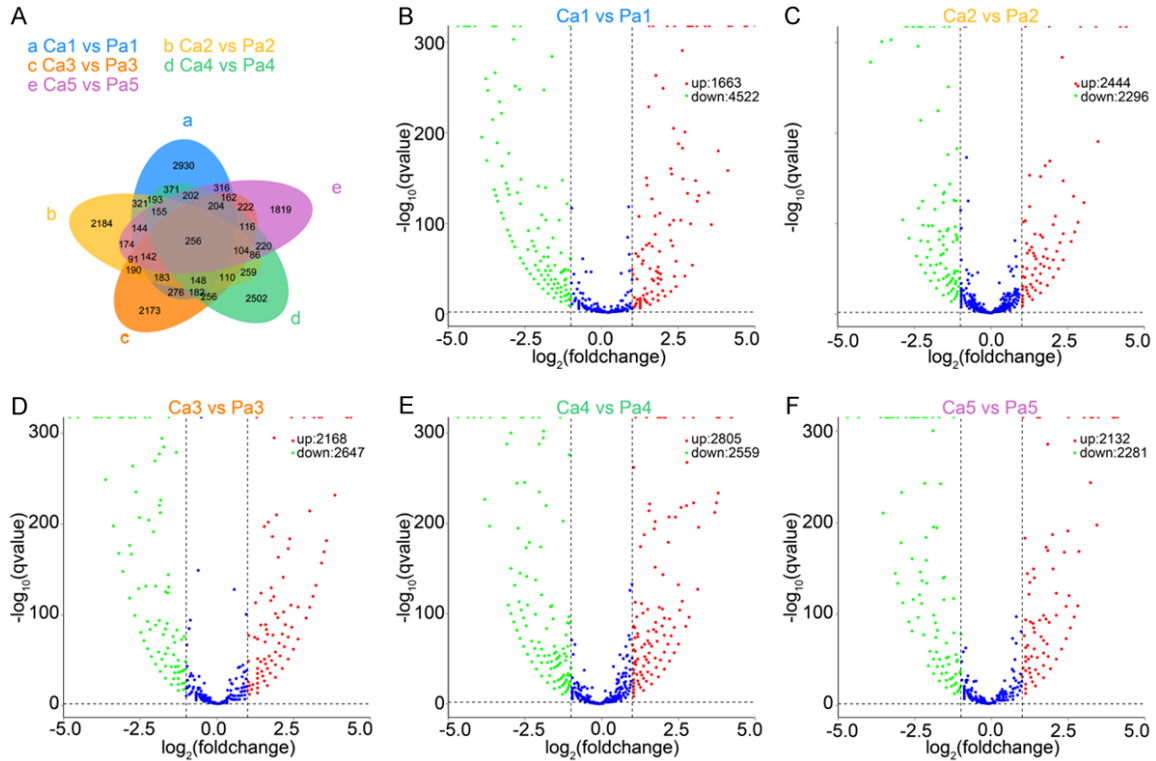


Figure 2. Analysis of co-differentially expressed circRNAs (co-DE_circRNAs) in five paired samples. A. Hierarchical clustering analysis of 256 co-DE_circRNAs in five paired samples. B-F. Volcano plots of downregulation and upregulation of all DE_circRNAs in each paired sample.

ing characteristic (ROC) curves were used to evaluate the diagnostic values of the circRNAs in LCs or LSCCs. All analyses were two-sided and P -value < 0.05 was considered statistically significant.

Results

Expression profiles of circRNAs via RNA-seq in LSCCs with adjacent normal paired tissues

The characteristics of circular RNA transcripts via RNA-seq analysis of rRNA-depleted RNA from 10 samples (five LSCCs and five adjacent normal paired tissues) are shown in **Figure 1**. The constructed RNA-seq libraries of each sample were sequenced with Illumina HiSeq, yielding more than 50 million reads mapping to the human reference genome (GRCH37/hg38). A computational pipeline based on anchor alignment and more than two back-spliced junctions of unmapped reads was applied to ascertain inferred circRNAs as previously described [25, 26]. A total of 16,893 predicted circRNAs by sequencing paired tissues was obtained. There were 10,289 novel circRNAs and 6,604

overlapped circRNAs in all predicted circRNAs in all lung samples according to the circBase website. The median of the circRNA length distribution was 998 nt (**Figure 1B**).

The inferred circRNAs were annotated to determine their characteristics. Approximately 80% of the circRNA host genome originated from exons, 8% from introns, and 12% from intergenic regions (**Figure 1C**). Read counts were used to normalize the expression of putative circRNAs using TPM. Read count_TPM of more than 80% circRNAs were 0-0.1 (**Figure 1D**). Aberrant expression analysis of numerous circRNAs indicated a specific expression landscape in five paired LSCC samples (**Figure 2A-F**). A total of 9,952 downregulated circRNAs and 9,202 upregulated circRNAs in all five paired samples were identified, as evaluated by volcano plots (**Figure 2B-F**). However, of all DE_circRNAs in matched tissues, there were only 256 co-differentially expressed circRNAs (co-DE_circRNAs) shown from hierarchical clustering analysis (**Figure 2A**), among which 15 were significantly co-upregulated and 93 were co-downregulated (**Supplementary Table 1**).

Circular RNA for lung squamous cell carcinomas diagnosis

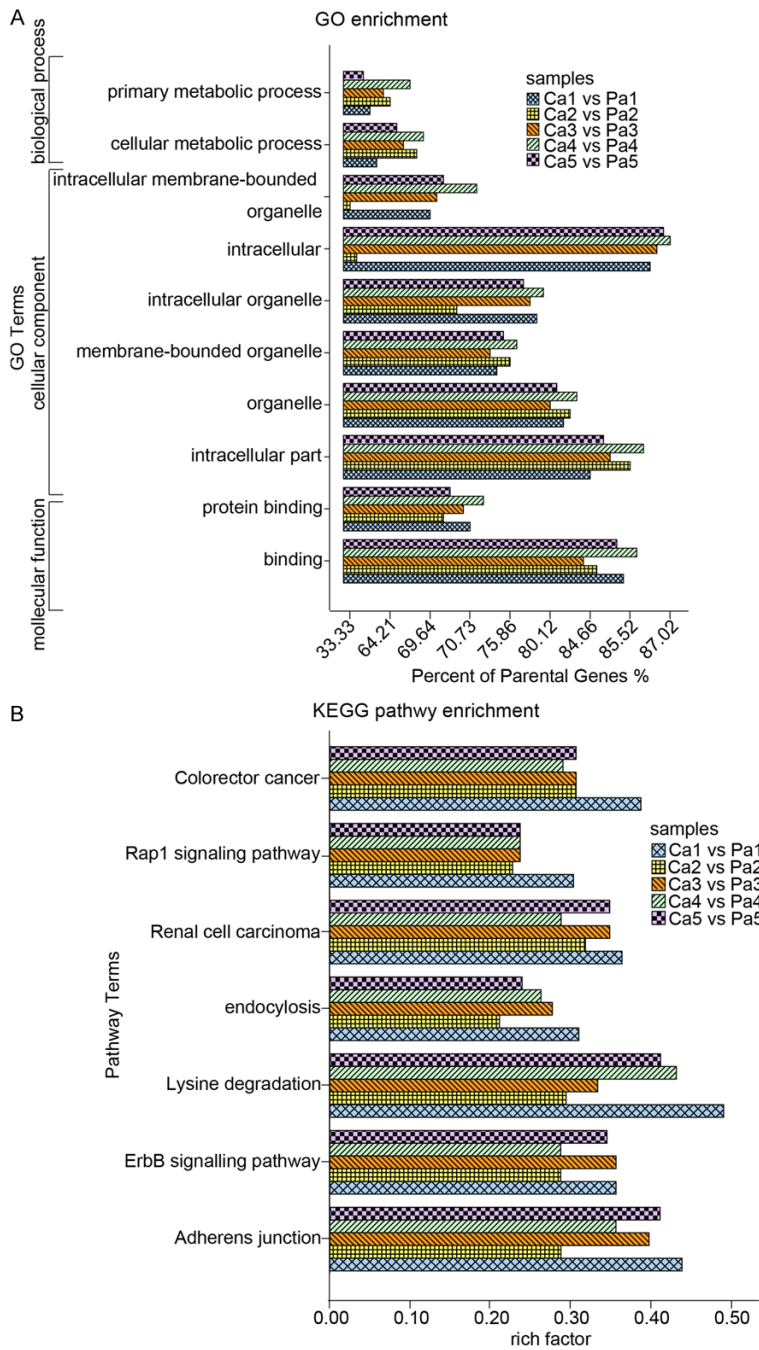


Figure 3. GO and KEGG pathways of co-enrichment analysis in five paired LSCC samples. A. Top 10 GO of co-enrichment analysis. B. Top 7 KEGG pathways of co-enrichment analysis.

Function assessments of circRNAs according to GO and KEGG pathway analysis

We used the GO and KEGG pathway enrichment analyses to systematically explore possible functions according to the parental genes of DE_circRNAs. The GO term types consist

of cellular component (CC), biological process (BP), and molecular function (MF). The top three functions of the parental genes were enriched mainly in protein binding of molecular function, intracellular part of cellular component, and metabolic process of biological process in turn (**Figure 3A, Supplementary Figure 2**). KEGG pathway analysis was performed based on q -value < 0.05 and rich factors. The closer the q -value is to zero, the higher the rich factor is, the more significantly the pathways are enriched by parental genes of DE_circRNAs. Of the top 20 significantly enriched pathways in five paired LSCCs, adherens junction, lysine degradation, and the ErbB signaling pathway were the three most enriched pathways sequentially (**Figure 3B, Supplementary Figure 3**) and were associated with NSCLCs [32, 33].

Identification of inferred DE_circRNAs by qRT-PCR with Sanger sequencing in lung cancer tissues

All 108 (15 up-regulated and 93 down-regulated) co-DE_circRNAs in five paired LSCCs originated from 108 (22 up + 86 down) assumed parental genes. PubMed was used as the search engine to study whether putative parental genes were associated with previous cancer studies. Five co-DE_circRNAs were chosen for verification in 86 lung samples (43 LC and 43 adjacent normal paired tissues). Only four of five co-DE_circRNAs were validated primarily via reverse transcription qPCR (qRT-PCR) (**Figure 4A-E**), the same trend as in RNA-seq data (**Figure 4F**). Sanger sequencing was performed to verify the primers and the cyclization sites of circRNAs (**Supplementary Figure 1**).

Circular RNA for lung squamous cell carcinomas diagnosis

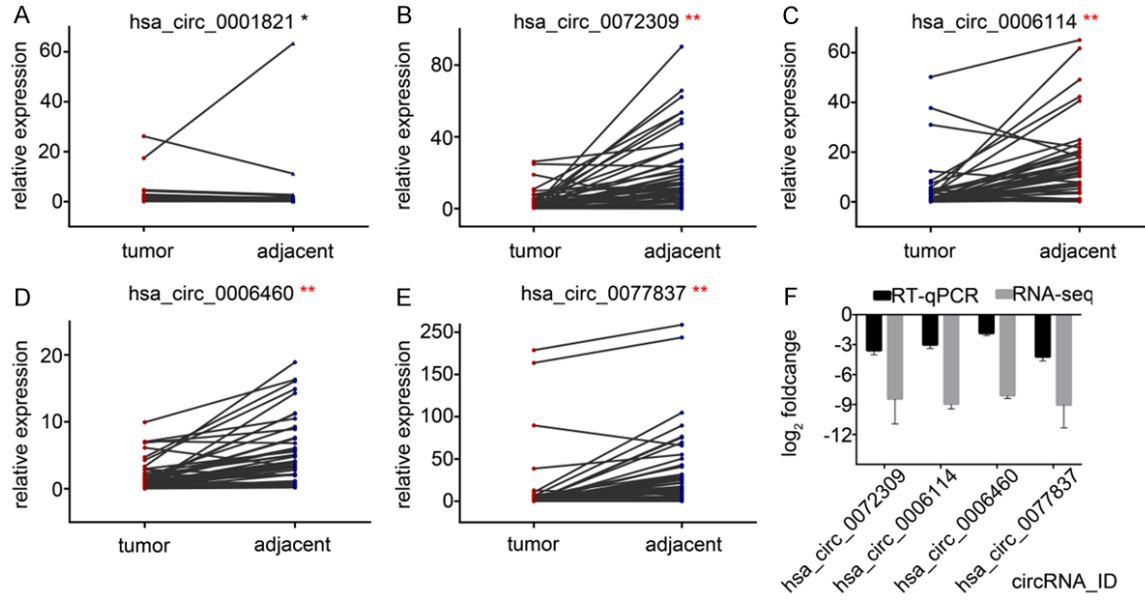


Figure 4. Identification of inferred DE_circRNAs in lung cancer samples by qRT-PCR, with the same trend as in RNA-seq. A-E. Identification of inferred DE_circRNAs in 86 samples (43 lung cancer and 43 paired adjacent non-tumor tissues) by qRT-PCR (normalized by GAPDH). F. qRT-PCR with the same trend as in RNA-seq of four identified circRNAs. * $P > 0.05$, ** $P < 0.01$.

Correlations between clinical features and circRNA expression levels ($2^{-\Delta\Delta Ct}$) in lung cancer

In order to exclude the possible effects of clinical features on the relative expression of each validated circRNA, clinical characteristics of LC subjects were portrayed first (Table 2). According to the classical pathological types of LC, there were 15 (34.88%) LSCCs, 19 (44.19%) LADCs, 3 (6.98%) mixed, and 6 (13.95%) other types of lung carcinomas. Mixed LC indicated no less than two histological patterns in one sample, such as adenosquamous and adeno- or squamous- with other types. Six other types in our registered patients included 3 neuroendocrine carcinomas, 2 large cell carcinomas, and 1 myoepithelial carcinoma. The stages of the 43 collected LCs were as follows: 39 (90.70%) IA1-III A and 4 (9.30%) IIIB-IV stages, according to the eighth edition of the TNM classification (TNM^{8th}) for LC in 2016 [34]. It was concluded that most LC samples were from males in early stages of LC. Furthermore, all female and two male patients were non-smokers. Most female nonsmokers had LADCs (6/7), while male smokers (34/36) had LSCCs (15/34), LADCs (12/34), and other subtypes.

Gender, age, smoking status, cancer family, TNM^{8th}, and blood CEA, CYFRA21-1, and NSE

were not associated with expression levels of the four validated co-DE_circRNAs in LC tissues (all $P > 0.05$), but the expression levels were associated with pathological types with statistical significance ($P < 0.05$). Specifically, pathological types had a significant correlation with three circRNAs excluding hsa_circ_0072309 (hsa_circ_0072309: $P = 0.068 > 0.05$; hsa_circ_0006114: $P = 0.013 < 0.05$; hsa_circ_0006460: $P = 0.035 < 0.05$; hsa_circ_0077837: $P = 0.001 < 0.01$, Spearman correlations). Hsa_circ_0072309 and hsa_circ_0006460 were both negatively correlated with blood SCC (hsa_circ_0072309: $P = 0.028 < 0.05$; hsa_circ_0077637: $P = 0.034 < 0.05$) (Table 3).

Diagnostic potential evaluation of inferred circRNAs in early stage lung cancer

To evaluate whether the validated circRNAs can serve as indicators for LC, the ROC curves were used and the area under the ROC curve (AUC) values were computed (Table 4, Figure 5). The highest AUC value of the four circRNAs of LCs was that of Hsa_circ_0072309 (AUC: 0.871) corresponding to a sensitivity 0.744 and a specificity 0.884. Combination of these four circRNAs produced a high AUC value (AUC: 0.871, Figure 7A), without corresponding in-

Circular RNA for lung squamous cell carcinomas diagnosis

Table 2. Clinical characteristics of lung cancer patients

Characteristics	Subgroup	Numbers of case (freq %)
Gender	Male	36 (83.72)
	Female	7 (16.28)
Age (year-old)	Mean ± SE: 57.95±1.16	
	≤50	10 (23.26)
	>50-60	17 (39.53)
	>60	16 (37.21)
Smoking status	Median (25%-75% quantile): 22.50 (5.00-40.00)	
	No smoking	9 (20.93)
	Smoking	34 (79.07)
Packs per year	>0-30	14 (32.56)
	>30-60	11 (25.58)
	>60	9 (20.93)
Cancer family	No	31 (72.09)
	Yes	12 (27.81)
	Lung cancer	4 (9.30)
	Other cancer	8 (18.60)
Pathological types	Squamous carcinoma	15 (34.88)
	Adenocarcinoma	19 (44.19)
	Mixed	3 (6.98)
	Others	6 (13.95)
TNM ^{8th}	I-III A	39 (90.70)
	IIIB-IV	4 (9.30)
SCC (<1.8 ng/ml)	No	36 (83.7)
	Yes	7 (16.3)
CEA (0-5 ug/L)	No	31 (72.1)
	Yes	12 (27.9)
NSE (0-24 ng/ml)	No	42 (97.7)
	Yes	1 (2.3)
CYFRA21-1 (0.1-4.0 ng/ml)	No	29 (67.4)
	Yes	13 (30.2)
	Missing	1 (2.4)

Table 3. Correlation between each circRNA expression and characteristics of lung cancer patients

Characteristics	P-values (coefficient) of each circRNA				
	01821	72309	06114	06460	77837
Gender	0.627	0.228	0.381	0.456	0.215
Age	0.993	0.603	0.168	0.490	0.317
Smoking status	0.660	0.182	0.410	0.444	0.173
Cancer family	0.955	0.305	0.119	0.226	0.125
Pathological types	0.241	0.068	0.013 (0.375*)	0.035 (0.322*)	0.001 (0.476*)
TNM ^{8th}	0.214	0.427	0.393	0.930	0.203
SCC (<1.8 ng/ml)	0.582	0.028 (-0.335*)	0.215	0.974	0.034 (-0.325*)
CEA (0-5 ug/L)	0.131	0.505	0.309	0.979	0.832
NSE (0-24 ng/ml)	0.475	0.937	0.300	0.874	0.475
CYFRA21-1 (0.1-4.0 ng/ml)	0.084	0.413	0.181	0.200	0.140

Notes: 01821: hsa_circ_0001821, 72309: hsa_circ_0072309, 06114: hsa_circ_0006114, 06460: hsa_circ_0006460, 77837: hsa_circ_0077837; (*): correlation coefficient.

Circular RNA for lung squamous cell carcinomas diagnosis

Table 4. AUC values of circRNAs in LCs

circRNA_ID	P-value	AUC (SE)	95% CI		Cutoff Value	Sensitivity (%)	Specificity (%)	Youden Index
			LB	UB				
Hsa_circ_0072309	$P < 0.001$	0.871 (0.039)	0.794	0.948	8.092	0.884	0.744	0.628
Hsa_circ_0006114	$P < 0.001$	0.821 (0.047)	0.730	0.912	6.109	0.860	0.721	0.581
Hsa_circ_0006460	$P < 0.001$	0.778 (0.051)	0.678	0.877	3.068	0.814	0.698	0.512
Hsa_circ_0077837	$P < 0.001$	0.861 (0.045)	0.774	0.948	9.023	0.860	0.814	0.674

Notes: AUC: area under the receiver operating characteristic curve; SE: standard error; 95% CI: 95% confidence interval; LB: lower Bound of 95% CI; UB: upper Bound of 95% CI; Cutoff: Cutoff value for diagnosis.

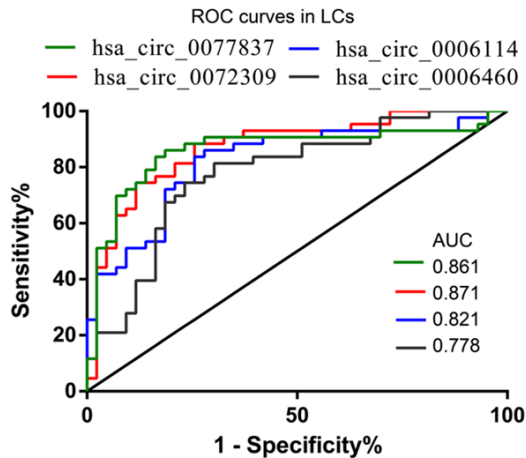


Figure 5. ROC curves in LCs.

crease in sensitivity (0.767) and specificity (0.837).

The diagnostic value of circRNAs in LSCCs was further assessed to discriminate from LADCs. According to the multiple comparison analyses based on the Kruskai-Wallis test, there was statistically differential expression in the four circRNAs between LADC, and LSCC subgroups ($P < 0.001$) (Figure 6A-E). Hsa_circ_0006460 was also significantly discriminated between squamous and mixed carcinoma subgroups. Other multiple comparisons of the four circRNA expression levels between any two pathological subtypes had no statistical difference ($P > 0.05$). Then, AUC values of the four circRNAs were found to be higher than 0.8; hsa_circ_0077837 showed the highest AUC value (0.947) with a higher sensitivity (0.867) and a specificity (0.947) (Table 5, Figure 6F). The combination of these four circRNAs did not presented a higher AUC value (AUC: 0.937, Figure 7B), with sensitivity of 0.933 and specificity of 0.867.

In summary, we first portrayed the landscape of circRNAs in LSCCs and validated the down-

regulation of four validated circRNAs in LCs (hsa_circ_0072309, hsa_circ_0006460, hsa_circ_0006114, hsa_circ_0077837). The protein binding of molecular function, intracellular part of cellular component, and metabolic process of biological process were the top three functions of circRNA parental genes, and adherens junction, lysine degradation, and ErbB signaling pathway were the three most enriched pathways. The downregulated expression levels of circRNAs also had statistical discrepancy regarding LSCCs discriminated from LADCs. Pathological types of LCs were associated with expression levels of three circRNAs, regardless of gender, age, smoking status, cancer family, TNM^{8th}, or blood CEA, NSE, and CYFRA21-1. Hsa_circ_0072309 and hsa_circ_0077837 were negatively correlated with blood SCC. Hsa_circRNA_0072309 and hsa_circ_0077837 may serve as biomarkers for the diagnosis of LCs and LSCCs, respectively.

Discussion

Early diagnosis of LC is very critical for improving the survival rate of the patients with lung cancer. The traditional biomarkers of LSCC (SCC and CYFRA 21-1) have relatively low sensitivity and specificity in the early stage of lung cancer. There are increasing evidence that cancer-related circRNAs are promising biomarkers for diagnosis, prognosis, and survival [15, 18, 20, 35]. Nevertheless, investigation of circRNAs as favorable tumor biomarkers of LC is incomplete and based on systemic research, most of which have focused on basic cell lines or tumor types other than LC, especially LSCCs. Therefore, features and functions of circRNAs in LC remained unclear.

Recently, Wang et al. demonstrated *circ-ITCH* expression and its characteristics in 76 Chinese LC patients [12]. Another team showed the overexpression of circRNA_100876 in NSCLC

Circular RNA for lung squamous cell carcinomas diagnosis

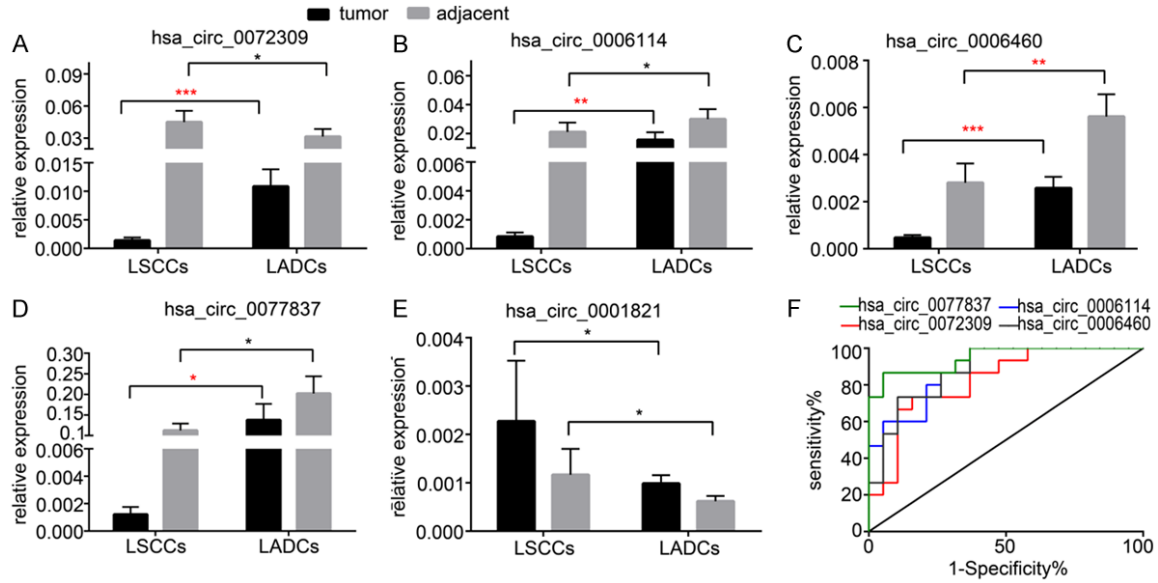


Figure 6. Identification of inferred DE_circRNAs in LSCCs discriminated from LADCs by qRT-PCR (A-E). Normalized by GAPDH and ROC curves of four identified DE_circRNAs in LSCCs (F). * $P > 0.05$, * $P < 0.05$, ** $P < 0.01$.

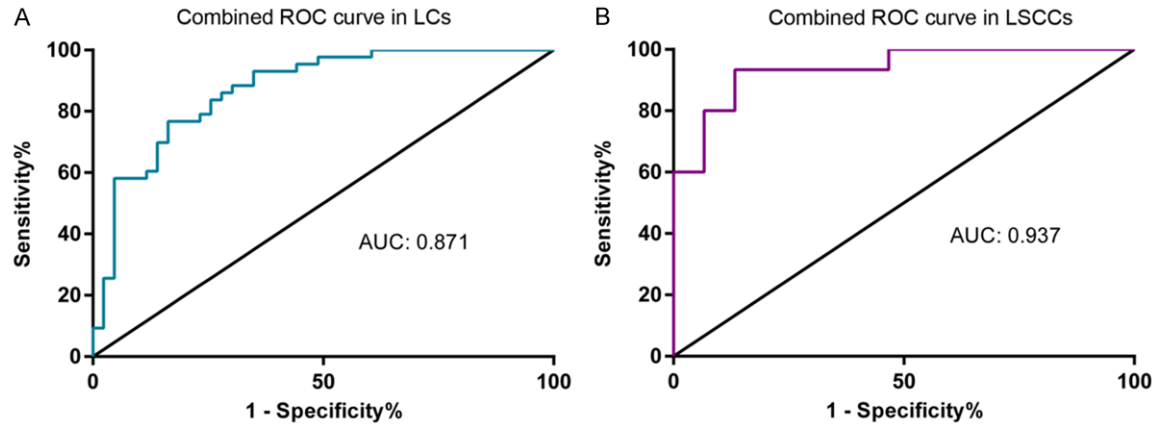


Figure 7. Combined ROC curves in LCs (A) and LSCCs (B).

Table 5. AUC values of circRNAs in LSCCs

circRNA_ID	P-value	AUC (SE)	95% CI		Cutoff Value	Sensitivity (%)	Specificity (%)	Youden Index
			LB	UB				
Hsa_circ_0072309	$P < 0.001$	0.825 (0.072)	0.684	0.965	0.842	0.733	0.744	0.575
Hsa_circ_0006114	$P < 0.001$	0.884 (0.055)	0.776	0.992	2.379	1.000	0.632	0.632
Hsa_circ_0006460	$P < 0.001$	0.881 (0.057)	0.768	0.993	2.006	1.000	0.632	0.632
Hsa_circ_0077837	$P < 0.001$	0.947 (0.036)	0.877	1.000	0.458	0.867	0.947	0.814

Notes: AUC: area under the receiver operating characteristic curve; SE: standard error; 95% CI: 95% confidence interval; LB: lower Bound of 95% CI; UB: upper Bound of 95% CI; Cutoff: Cutoff value for diagnosis.

and its prognostic value [35]. However, both groups studied only a single circRNA identified by previous investigators, and the results were

not consistent with this study. We reported a profiling study from the circRNA perspective in human LC though RNA-seq and bioinformatics

technology. We profiled several DE_circRNAs in five paired tissues of surgical LSCC samples and identified four co-DE_circRNAs tentatively. Functional prediction of DE_circRNAs was also performed on the basis of the GO and KEGG analyses. Correlation with clinical characteristics were assessed. To our knowledge, this is the first study where four circRNAs were identified as diagnostic biomarkers in LC, although their specific properties in LC still remain unclear.

We initially profiled the landscape of circRNAs and annotated them in 10 samples, and then filtered DE_circRNAs in LCs with paired adjacent normal tissues according to RNA-seq and demonstrated five circRNAs in 86 samples (hsa_circ_0001821, hsa_circ_0072309, hsa_circ_0006114, hsa_circ_006460, hsa_circ_0077837). Our results indicate that four of the five circRNAs were downregulated in LCs and distinguished from corresponding paired samples with respective multiples (hsa_circ_0072309: 5.603-fold, hsa_circ_0006114: 3.235-fold, hsa_circ_006460: 2.924-fold, hsa_circ_0077837: 2.846-fold).

The functions of the five circRNAs remain unclear, although their parental genes might be involved in cancer generation and progress. The parental gene of hsa_circ_0072309, named *circLIFR*, is leukemia inhibitory factor receptor (*LIFR*), which was demonstrated to be a metastasis suppressor and prognostic biomarker in abundant tumors, such as in hepatocellular and pancreatic cancer [36, 37]. Investigators have not clarified the relationship between *LIFR* and LC so far, albeit *LIFR* is distributed in lung and bronchial epithelium [38, 39]. Another circRNA (hsa_circ_0006114) parental gene, protein tyrosine phosphatase- μ (*PTPRM*), might regulate cancer cell migration in A549 cell lines [40]. *PTPRM* is a tumor suppressor contributing to colonic tumorigenesis [41] and is negatively associated with disease prognosis for breast cancer [42]. Therefore, *PTPRM* demonstrates a variety of characteristics in different types of cancer. The parental gene of the third circRNA, namely *circEPB41L2*, is one of the skeletal protein 4.1 (*EPB41*) gene family members (erythrocyte protein 4.1G, *EPB41L2*). The protein level of 4.1G was found to be significantly lower in NSCLCs with relation to tumor cell differentiation [43]. The functions of the three circRNAs mentioned above are not clear

yet. We verified their downregulation of expression and diagnostic value in LCs, especially in LSCCs. It is well known that the *BRAF* gene is one of the oncogenic drivers of NSCLC and SCLC. Hsa_circ_006460, termed *circBRAF*, might serve as a diagnostic biomarker for LCs in our study, consistent with that in glioma patients [22]. *PVT1*, one of the long non-coding RNAs, was identified as a potential target marker for diagnosis and poor prognosis in LCs in a previous study [44]. However, hsa_circ_0001821, named *circPVT1*, as a prognostic marker of gastric cancer [20], did not exhibit statistically different expression in our LC samples compared with in adjacent normal tissues.

We then assessed the correlations between circRNA expression levels and the clinical characteristics, and the diagnostic ability of circRNAs in early stage LCs. Three of the four circRNA expression levels were statistically associated with tumor pathological subsets (LADC and LSCC) (*circPTPRM*, *circBRAF*, and *circEPB41L2*: $r = 0.375, 0.322, 0.476$, respectively). *CircLIFR* and *circEPB41L2* were negatively associated with blood SCC as well. *circLIFR* exhibited a suitable diagnosis value for LCs (the highest AUC value of four circRNAs: 0.871, sensitivity: 0.744, specificity: 0.884), as did *circEPB41L2* for LSCCs (AUC value: 0.947, sensitivity: 0.867, specificity: 0.947), indicating that these circRNAs could be appropriate diagnosis biomarkers for LCs or LSCCs.

Finally, the putative functions and enrichment of DE_circRNAs were systematically assessed using GO and KEGG using their parental genes. The top three functions of the source genes were enriched mainly in the protein binding of molecular function, intracellular part of cellular component, and metabolic process of biological process, in turn, based on GO functional prediction. The results were consistent with previous reports [5-9]. The three most enriched pathways were filtered from the top 20 most significant ones in five paired LSCCs: adherens junction, lysine degradation, and ErbB signaling pathway. A number of investigators found that the loss of cell-to-cell adhesion was critical to drive cancer cell proliferation and migration via repressing cell adhesion molecules in LC [32]. Lysine degradation is one of the famous metabolic pathways, but it is unclear as how lysine degradation plays a role in LC. ErbB signaling

pathway has been investigated extensively and is involved in cancer-associated signaling pathways including in LC [33]. The functional enrichment of circRNAs in LC should be studied further to validate the roles of circRNAs in LC development.

In conclusion, the landscape of circRNAs and the function assessments of Chinese LSCCs were profiled. The downregulation of expression of the four circRNAs was significantly different in LC (*circLIFR*, *circBRAF*, *circPTPRM*, and *circEPB41L2*) and associated with pathological types. *CircLIFR* and *circEPB41L2* had a negative correlation with blood SCC. Hence, the four circRNAs may serve as diagnostic biomarkers for LCs, or even LSCCs. However, additional investigative efforts are needed to confirm our findings with additional samples.

Acknowledgements

No grants. We wish to thank Jian-Tao Pu for help with the manuscript correction and Novogene Science and Technology Co. Ltd. for help with next-generation sequencing.

Disclosure of conflict of interest

None.

Address correspondence to: Dr. Liang-An Chen, Medical School, Nankai University, Tianjin 300071, P.R. China; Department of Respiratory Medicine, Chinese PLA General Hospital, 28 Fuxing Rd, Haidian Dist, Beijing 100853, P.R. China. Tel: +86-10-55499327; E-mail: chenliangan301@163.com

References

- [1] Chen W, Zheng R, Baade PD, Zhang S, Zeng H, Bray F, Jemal A, Yu XQ and He J. Cancer statistics in China, 2015. *CA Cancer J Clin* 2016; 66: 115-132.
- [2] Mulshine JL and Sullivan DC. Clinical practice. Lung cancer screening. *N Engl J Med* 2005; 352: 2714-2720.
- [3] Zamay TN, Zamay GS, Kolovskaya OS, Zukov RA, Petrova MM, Gargaun A, Berezovski MV and Kichkailo AS. Current and prospective protein biomarkers of lung cancer. *Cancers (Basel)* 2017; 9: 155.
- [4] Ma R, Xu H, Wu J, Sharma A, Bai S, Dun B, Jing C, Cao H, Wang Z, She JX and Feng J. Identification of serum proteins and multivariate models for diagnosis and therapeutic monitoring of lung cancer. *Oncotarget* 2017; 8: 18901-18913.
- [5] Du WW, Yang W, Liu E, Yang Z, Dhaliwal P and Yang BB. Foxo3 circular RNA retards cell cycle progression via forming ternary complexes with p21 and CDK2. *Nucleic Acids Res* 2016; 44: 2846-2858.
- [6] Li Z, Huang C, Bao C, Chen L, Lin M, Wang X, Zhong G, Yu B, Hu W, Dai L, Zhu P, Chang Z, Wu Q, Zhao Y, Jia Y, Xu P, Liu H and Shan G. Exon-intron circular RNAs regulate transcription in the nucleus. *Nat Struct Mol Biol* 2015; 22: 256-264.
- [7] Hansen TB, Jensen TI, Clausen BH, Bramsen JB, Finsen B, Damgaard CK and Kjems J. Natural RNA circles function as efficient microRNA sponges. *Nature* 2013; 495: 384-388.
- [8] Zheng Q, Bao C, Guo W, Li S, Chen J, Chen B, Luo Y, Lyu D, Li Y, Shi G, Liang L, Gu J, He X and Huang S. Circular RNA profiling reveals an abundant circHIPK3 that regulates cell growth by sponging multiple miRNAs. *Nat Commun* 2016; 7: 11215.
- [9] You X, Vlatkovic I, Babic A, Will T, Epstein I, Tushev G, Akbalik G, Wang M, Glock C, Quedenau C, Wang X, Hou J, Liu H, Sun W, Sambandan S, Chen T, Schuman EM and Chen W. Neural circular RNAs are derived from synaptic genes and regulated by development and plasticity. *Nat Neurosci* 2015; 18: 603-610.
- [10] Wilusz JE and Sharp PA. Molecular biology. A circuitous route to noncoding RNA. *Science* 2013; 340: 440-441.
- [11] Yang Y, Fan X, Mao M, Song X, Wu P, Zhang Y, Jin Y, Yang Y, Chen LL, Wang Y, Wong CC, Xiao X and Wang Z. Extensive translation of circular RNAs driven by N(6)-methyladenosine. *Cell Res* 2017; 27: 626-641.
- [12] Wan L, Zhang L, Fan K, Cheng ZX, Sun QC and Wang JJ. Circular RNA-ITCH suppresses lung cancer proliferation via inhibiting the wnt/beta-catenin pathway. *Biomed Res Int* 2016; 2016: 1579490.
- [13] Yao Z, Luo J, Hu K, Lin J, Huang H, Wang Q, Zhang P, Xiong Z, He C, Huang Z, Liu B and Yang Y. ZKSCAN1 gene and its related circular RNA (*circZKSCAN1*) both inhibit hepatocellular carcinoma cell growth, migration, and invasion but through different signaling pathways. *Mol Oncol* 2017; 11: 422-437.
- [14] He J, Xie Q, Xu H, Li J and Li Y. Circular RNAs and cancer. *Cancer Lett* 2017; 396: 138-144.
- [15] Zhang Y, Liang W, Zhang P, Chen J, Qian H, Zhang X and Xu W. Circular RNAs: emerging cancer biomarkers and targets. *J Exp Clin Cancer Res* 2017; 36: 152.
- [16] Du WW, Fang L, Yang W, Wu N, Awan FM, Yang Z and Yang BB. Induction of tumor apoptosis through a circular RNA enhancing Foxo3 activity. *Cell Death Differ* 2017; 24: 357-370.
- [17] Xia W, Qiu M, Chen R, Wang S, Leng X, Wang J, Xu Y, Hu J, Dong G, Xu PL and Yin R. Circular

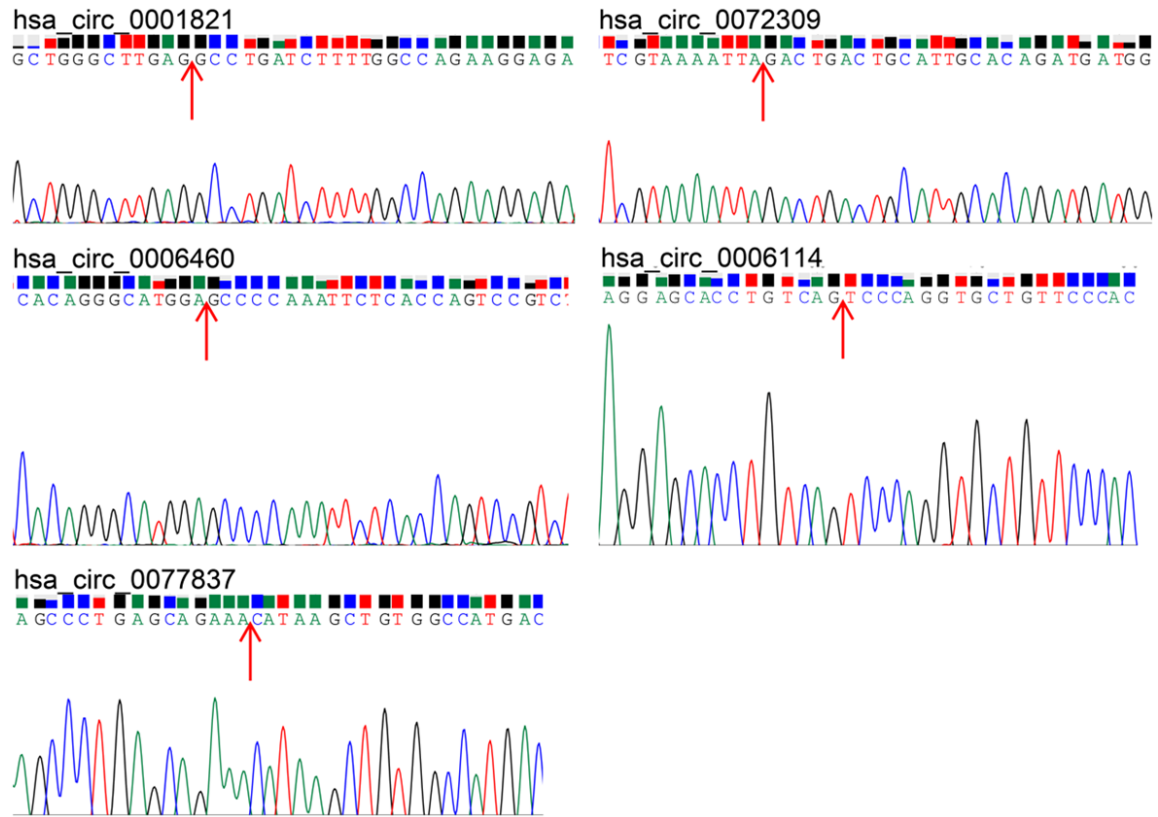
Circular RNA for lung squamous cell carcinomas diagnosis

- RNA has_circ_0067934 is upregulated in esophageal squamous cell carcinoma and promoted proliferation. *Sci Rep* 2016; 6: 35576.
- [18] Chen S, Li T, Zhao Q, Xiao B and Guo J. Using circular RNA hsa_circ_0000190 as a new biomarker in the diagnosis of gastric cancer. *Clin Chim Acta* 2017; 466: 167-171.
- [19] Li P, Chen H, Chen S, Mo X, Li T, Xiao B, Yu R and Guo J. Circular RNA 0000096 affects cell growth and migration in gastric cancer. *Br J Cancer* 2017; 116: 626-633.
- [20] Chen J, Li Y, Zheng Q, Bao C, He J, Chen B, Lyu D, Zheng B, Xu Y, Long Z, Zhou Y, Zhu H, Wang Y, He X, Shi Y and Huang S. Circular RNA profile identifies circPVT1 as a proliferative factor and prognostic marker in gastric cancer. *Cancer Lett* 2017; 388: 208-219.
- [21] Li Y, Zheng Q, Bao C, Li S, Guo W, Zhao J, Chen D, Gu J, He X and Huang S. Circular RNA is enriched and stable in exosomes: a promising biomarker for cancer diagnosis. *Cell Res* 2015; 25: 981-984.
- [22] Zhu J, Ye J, Zhang L, Xia L, Hu H, Jiang H, Wan Z, Sheng F, Ma Y, Li W, Qian J and Luo C. Differential expression of circular RNAs in glioblastoma multiforme and its correlation with prognosis. *Transl Oncol* 2017; 10: 271-279.
- [23] Langmead B, Trapnell C, Pop M and Salzberg SL. Ultrafast and memory-efficient alignment of short DNA sequences to the human genome. *Genome Biol* 2009; 10: R25.
- [24] Kim D, Pertea G, Trapnell C, Pimentel H, Kelley R and Salzberg SL. TopHat2: accurate alignment of transcriptomes in the presence of insertions, deletions and gene fusions. *Genome Biol* 2013; 14: R36.
- [25] Memczak S, Jens M, Elefsinioti A, Torti F, Krueger J, Rybak A, Maier L, Mackowiak SD, Gregersen LH, Munschauer M, Loewer A, Ziebold U, Landthaler M, Kocks C, Ie Noble F and Rajewsky N. Circular RNAs are a large class of animal RNAs with regulatory potency. *Nature* 2013; 495: 333-338.
- [26] Zhou L, Chen J, Li Z, Li X, Hu X, Huang Y, Zhao X, Liang C, Wang Y, Sun L, Shi M, Xu X, Shen F, Chen M, Han Z, Peng Z, Zhai Q, Chen J, Zhang Z, Yang R, Ye J, Guan Z, Yang H, Gui Y, Wang J, Cai Z and Zhang X. Integrated profiling of microRNAs and mRNAs: microRNAs located on Xq27.3 associate with clear cell renal cell carcinoma. *PLoS One* 2010; 5: e15224.
- [27] Love MI, Huber W and Anders S. Moderated estimation of fold change and dispersion for RNA-seq data with DESeq2. *Genome Biol* 2014; 15: 550.
- [28] Young MD, Wakefield MJ, Smyth GK and Oshlack A. Gene ontology analysis for RNA-seq: accounting for selection bias. *Genome Biol* 2010; 11: R14.
- [29] Kanehisa M, Araki M, Goto S, Hattori M, Hirakawa M, Itoh M, Katayama T, Kawashima S, Okuda S, Tokimatsu T and Yamanishi Y. KEGG for linking genomes to life and the environment. *Nucleic Acids Res* 2008; 36: D480-484.
- [30] Mao X, Cai T, Olyarchuk JG and Wei L. Automated genome annotation and pathway identification using the KEGG Orthology (KO) as a controlled vocabulary. *Bioinformatics* 2005; 21: 3787-3793.
- [31] Schmittgen TD and Livak KJ. Analyzing real-time PCR data by the comparative C(T) method. *Nat Protoc* 2008; 3: 1101-1108.
- [32] Kim A, Kim EY, Cho EN, Kim HJ, Kim SK, Chang J, Ahn CM and Chang YS. Notch1 destabilizes the adherens junction complex through upregulation of the snail family of E-cadherin repressors in non-small cell lung cancer. *Oncol Rep* 2013; 30: 1423-1429.
- [33] Hynes NE and MacDonald G. ErbB receptors and signaling pathways in cancer. *Curr Opin Cell Biol* 2009; 21: 177-184.
- [34] Goldstraw P, Chansky K, Crowley J, Rami-Porta R, Asamura H, Eberhardt WE, Nicholson AG, Groome P, Mitchell A, Bolejack V; International Association for the Study of Lung Cancer Staging and Prognostic Factors Committee, Advisory Boards, and Participating Institutions; International Association for the Study of Lung Cancer Staging and Prognostic Factors Committee Advisory Boards and Participating Institutions. The IASLC lung cancer staging project: proposals for revision of the TNM stage groupings in the forthcoming (eighth) edition of the TNM classification for lung cancer. *J Thorac Oncol* 2016; 11: 39-51.
- [35] Yao JT, Zhao SH, Liu QP, Lv MQ, Zhou DX, Liao ZJ and Nan KJ. Over-expression of CircRNA_100876 in non-small cell lung cancer and its prognostic value. *Pathol Res Pract* 2017; 213: 453-456.
- [36] Luo Q, Wang C, Jin G, Gu D, Wang N, Song J, Jin H, Hu F, Zhang Y, Ge T, Huo X, Chu W, Shu H, Fang J, Yao M, Gu J, Cong W and Qin W. LIFR functions as a metastasis suppressor in hepatocellular carcinoma by negatively regulating phosphoinositide 3-kinase/AKT pathway. *Carcinogenesis* 2015; 36: 1201-1212.
- [37] Ma D, Jing X, Shen B, Liu X, Cheng X, Wang B, Fu Z, Peng C and Qiu W. Leukemia inhibitory factor receptor negatively regulates the metastasis of pancreatic cancer cells in vitro and in vivo. *Oncol Rep* 2016; 36: 827-836.
- [38] Knight DA, Lydell CP, Zhou D, Weir TD, Robert Schellenberg R and Bai TR. Leukemia inhibito-

Circular RNA for lung squamous cell carcinomas diagnosis

- ry factor (LIF) and LIF receptor in human lung. Distribution and regulation of LIF release. *Am J Respir Cell Mol Biol* 1999; 20: 834-841.
- [39] Ikezono T, Wu T, Yao XL, Levine S, Logun C, Angus CW and Shelhamer JH. Leukemia inhibitory factor induces the 85-kDa cytosolic phospholipase A2 gene expression in cultured human bronchial epithelial cells. *Biochim Biophys Acta* 1997; 1355: 121-130.
- [40] Hyun SW, Anglin IE, Liu A, Yang S, Sorkin JD, Lillehoj E, Tonks NK, Passaniti A and Goldblum SE. Diverse injurious stimuli reduce protein tyrosine phosphatase- μ expression and enhance epidermal growth factor receptor signaling in human airway epithelia. *Exp Lung Res* 2011; 37: 327-343.
- [41] Sudhir PR, Lin ST, Chia-Wen C, Yang SH, Li AF, Lai RH, Wang MJ, Chen YT, Chen CF, Jou YS and Chen JY. Loss of PTPRM associates with the pathogenic development of colorectal adenoma-carcinoma sequence. *Sci Rep* 2015; 5: 9633.
- [42] Sun PH, Ye L, Mason MD and Jiang WG. Protein tyrosine phosphatase micro (PTP micro or PTPRM), a negative regulator of proliferation and invasion of breast cancer cells, is associated with disease prognosis. *PLoS One* 2012; 7: e50183.
- [43] Zheng XY, Qi YM, Gao YF, Wang XY, Qi MX, Shi XF and An XL. [Expression and significance of membrane skeleton protein 4.1 family in non-small cell lung cancer]. *Ai Zheng* 2009; 28: 679-684.
- [44] Wang M, Ma X, Zhu C, Guo L, Li Q, Liu M and Zhang J. The prognostic value of long non coding RNAs in non small cell lung cancer: a meta-analysis. *Oncotarget* 2016; 7: 81292-81304.

Circular RNA for lung squamous cell carcinomas diagnosis



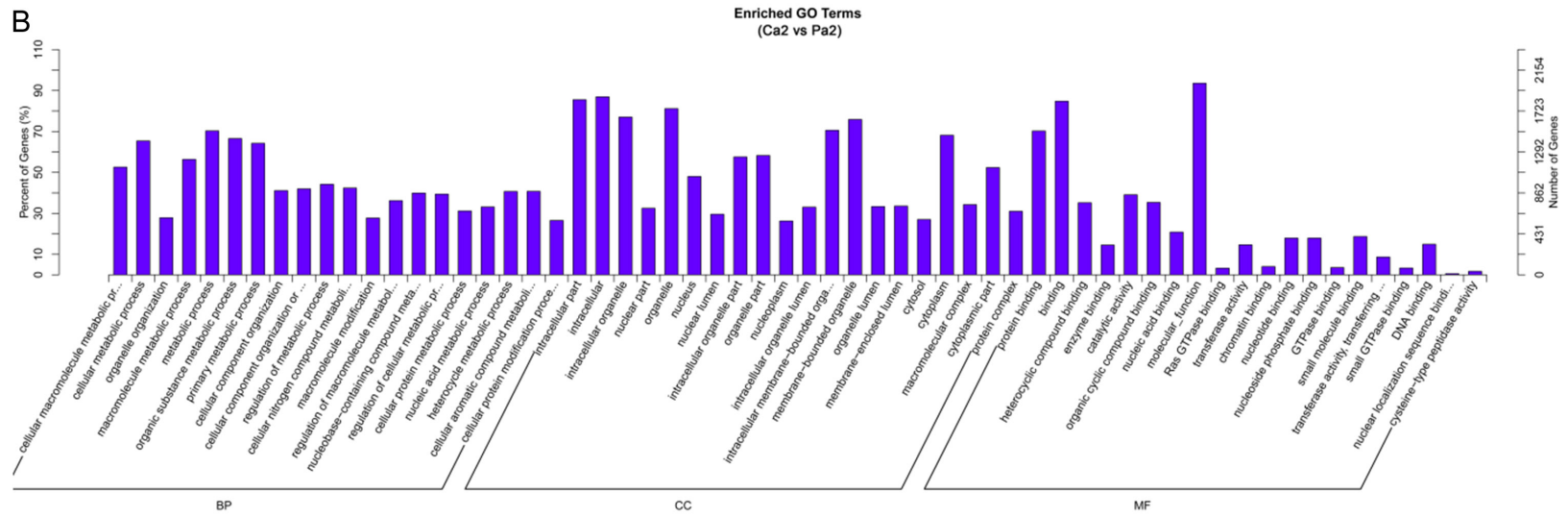
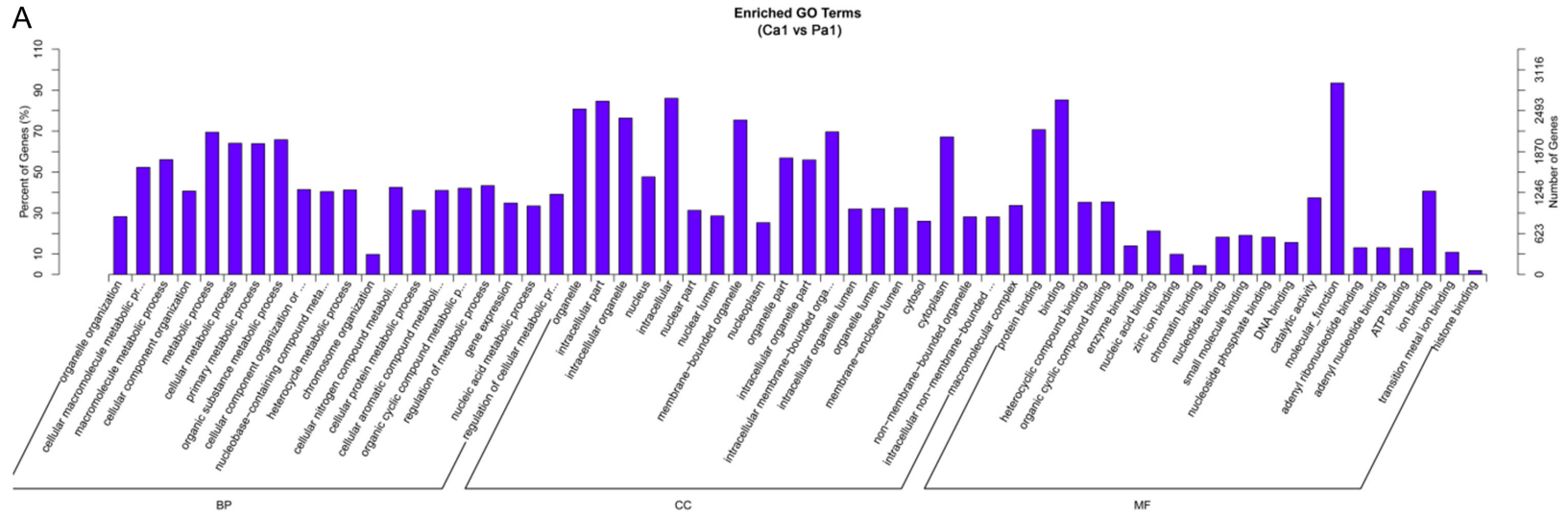
Supplementary Figure 1. Sanger sequencing information of five circRNAs. Red arrow indicates cyclization site of each circRNA.

Circular RNA for lung squamous cell carcinomas diagnosis

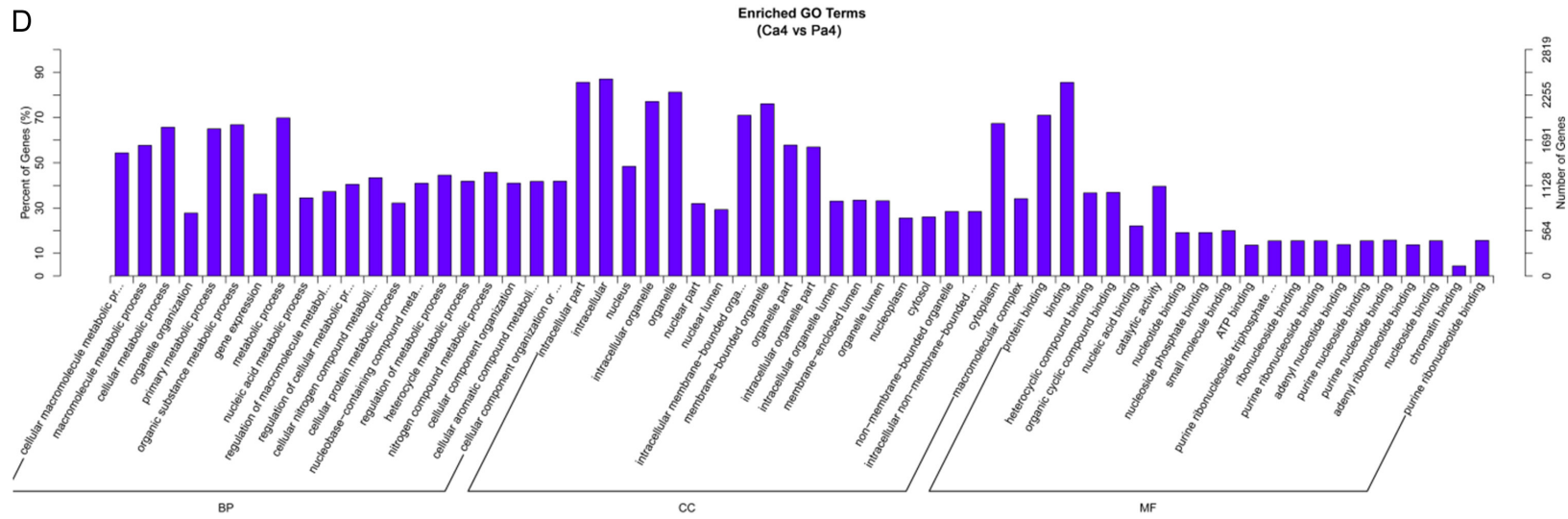
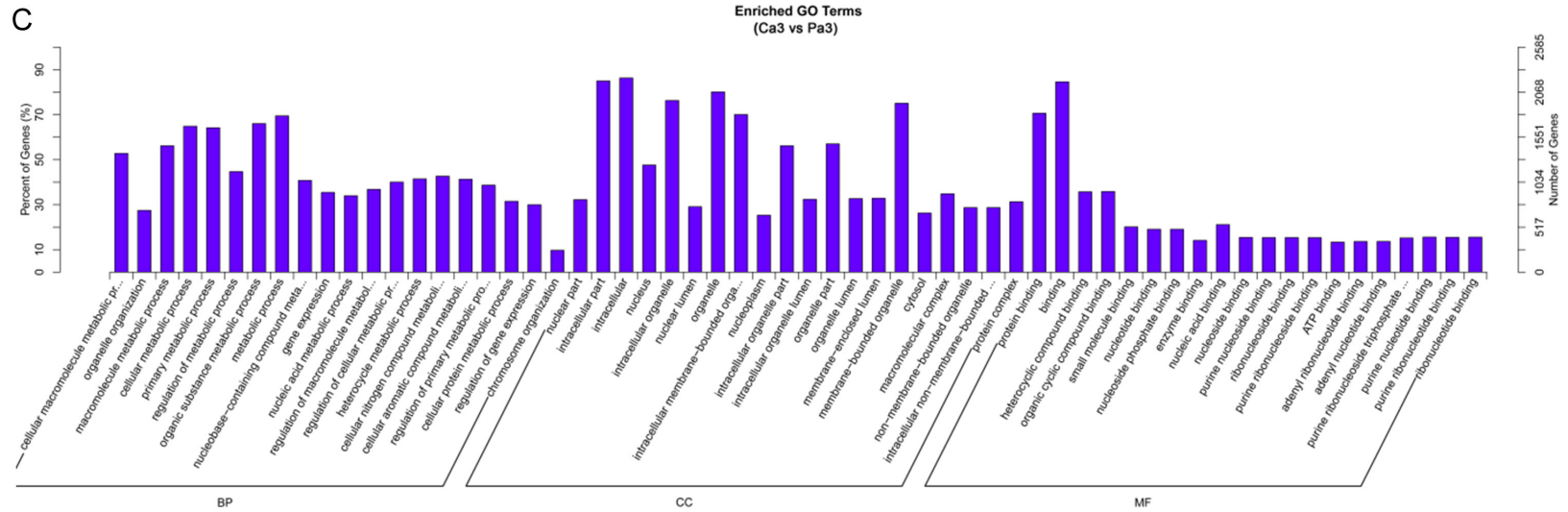
Supplementary Table 1. Upregulated and downregulated co-DE_circRNAs

Upregulated		Downregulated	
hg38_circ_0002203	hsa_circ_0077837	hg38_circ_0006619	hg38_circ_0011973
hg38_circ_0003610	hg38_circ_0013903	hg38_circ_0004554	hg38_circ_0015159
hg38_circ_0003609	hg38_circ_0009591	hg38_circ_0004551	hsa_circ_0056280
hg38_circ_0009240	hsa_circ_0000348	hsa_circ_0001613	hsa_circ_0047720
hsa_circ_0085173	hg38_circ_0005157	hg38_circ_0004568	hg38_circ_0003499
hsa_circ_0063809	hg38_circ_0012535	hsa_circ_0001648	hsa_circ_0001806
hsa_circ_0013218	hg38_circ_0006305	hg38_circ_0006568	hg38_circ_0000556
hg38_circ_0016015	hg38_circ_0006303	hsa_circ_0003353	hg38_circ_0011898
hsa_circ_0000766	hg38_circ_0002430	hsa_circ_0026782	hg38_circ_0012904
hg38_circ_0013877	hg38_circ_0002433	hsa_circ_0001936	hsa_circ_0000038
hsa_circ_0001821	hsa_circ_0072309	hg38_circ_0000381	hsa_circ_0008731
hsa_circ_0001238	hg38_circ_0013891	hsa_circ_0061774	hg38_circ_0012586
hsa_circ_0004543	hg38_circ_0006321	hg38_circ_0014988	hsa_circ_0024834
hsa_circ_0000768	hsa_circ_0093343	hsa_circ_0000369	hsa_circ_0006693
hg38_circ_0013878	hg38_circ_0011841	hg38_circ_0005386	hg38_circ_0011189
	hg38_circ_0016283	hg38_circ_0012903	hsa_circ_0008216
	hg38_circ_0006304	hsa_circ_0054558	hsa_circ_0001617
	hsa_circ_0006834	hsa_circ_0006376	hsa_circ_0003459
	hsa_circ_0003176	hsa_circ_0006460	hsa_circ_0001953
	hsa_circ_0002872	hsa_circ_0016123	hg38_circ_0016600
	hg38_circ_0006300	hsa_circ_0078299	hsa_circ_0008234
	hsa_circ_0058495	hsa_circ_0003310	hsa_circ_0004689
	hg38_circ_0010286	hg38_circ_0013130	hsa_circ_0005692
	hg38_circ_0008269	hsa_circ_0003587	hsa_circ_0002454
	hsa_circ_0001320	hsa_circ_0000702	hsa_circ_0058493
	hg38_circ_0009740	hsa_circ_0001236	hsa_circ_0001523
	hg38_circ_0000704	hsa_circ_0054214	hsa_circ_0005941
	hsa_circ_0006114	hg38_circ_0000920	hsa_circ_0001529
	hsa_circ_0005204	hg38_circ_0010139	hsa_circ_0001640
	hsa_circ_0008518	hg38_circ_0004558	hg38_circ_0002426
	hsa_circ_0007443	hg38_circ_0011739	hsa_circ_0008832
	hsa_circ_0077837	hg38_circ_0006619	hg38_circ_0011973

Circular RNA for lung squamous cell carcinomas diagnosis



Circular RNA for lung squamous cell carcinomas diagnosis



Circular RNA for lung squamous cell carcinomas diagnosis

